Earthquakes and Structures, *Vol. 7, No. 3 (2014) 333-347*
DOI: http://dx.doi.org/10.12989/eas.2014.7.3.333

Investigation of elasto-plastic seismic response analysis method for complex steel bridges

Zhanzhan Tang[1], Xu Xie*[1], Yan Wang[2], Junzhe Wang[3]

[1]*Department of Architecture & Civil Engineering*, *Zhejiang University*, *China*
[2]*College of Civil Engineering & Architecture*, *Zhejiang Sci-Tech University*, *China*
[3]*Department of Architecture & Civil Engineering*, *University of Bath*, *UK*

(Received February 18, 2014, Revised March 19, 2014, Accepted April 13, 2014)

Abstract. Multi-scale model can take both computational efficiency and accuracy into consideration when it is used to conduct elasto-plastic seismic response analysis for complex steel bridges. This paper proposed a method based on pushover analysis of member sharing the same section pattern to verify the accuracy of multi-scale model. A deck-through type steel arch bridge with a span length of 200m was employed for seismic response analysis using multi-scale model and fiber model respectively, the validity and necessity of elasto-plastic seismic analysis for steel bridge by multi-scale model was then verified. The results show that the convergence of load-displacement curves obtained from pushover analysis for members having the same section pattern can be used as a proof of the accuracy of multi-scale model. It is noted that the computational precision of multi-scale model can be guaranteed when length of shell element segment is 1.40 times longer than the width of section where was in compression status. Fiber model can only be used for the predictions of the global deformations and the approximate positions of plastic areas on steel structures. However, it cannot give exact prediction on the distribution of plastic areas and the degree of the plasticity.

Keywords: multi-scale model; fiber model; pushover analysis; complex steel bridge; elasto-plastic seismic response

1. Introduction

The design and evaluation of complex steel bridge under seismic loading especially for strong ground motions attract extensive concerns from various researchers. Nonaka (2001), Liang (2010), Usami (2004a, 2004b), Cetinkaya (2006), Xie (2012) have conducted elasto-plastic time history analysis on steel arch bridges or steel tower of suspension bridges using fiber models, and discussed the seismic performance and damage of complex steel bridges. However, all the analytical models in existing studies are fiber models, which cannot simulate the failure process of plastic areas on steel bridges accurately, so the computational accuracy requires verifications from other evaluation methods, and the seismic assessment results need further reviews.

Apart from unseating of girders and the failure of bearings, seismic damage of steel bridges can be mainly classified into four types according to many seismic disasters and test results

*Corresponding author, Professor, E-mail: xiexu@zju.edu.cn

http://www.techno-press.org/?journal=eas&subpage=7 ISSN: 2092-7614 (Print), 2092-7622 (Online)

(Kawashima 1997, Zheng 2000, Usami 2007, Ge 2009, Japanese Specifications 2002):

1) Local buckling or shear buckling of steel plates;
2) Global instability of the structure;
3) Residual deformation caused by exaggerated plastic strain;
4) Brittle failure caused by cumulative plastic strain.

In order to simulate the seismic damage process of steel bridge accurately, not only geometric nonlinearity should be considered in the analytical model, but also the local buckling of steel plates should be taken into account. Fiber model can hardly simulate the characteristics of seismic damage of the structures since it's unable to take the influence of local deformation of steel plates into consideration. Though shell model has a better performance on simulating local buckling and deformation of steel plates precisely and shows a great advantage in seismic analysis of complex steel bridges, the main drawback is its poor computational efficiency which makes it difficult to be applied in engineering practice.

The positions of seismic damaged areas are generally limited to certain parts of a steel bridge (Nonaka 2001, Usami 2007 and Alvarez 2012). Therefore, the no damaged or slightly damaged parts of a steel bridge can be modeled by fiber elements, while the seriously damaged parts can be modeled by shell elements, then the computational accuracy and efficiency can be significantly improved. The multi-scale model which consists of different types of elements is an improved model that can maintain both good computational efficiency and excellent accuracy. Although there have been many applications of multi-scale model in static and dynamic analysis of steel column members (Goto 1998, Ge 2000, Usami 2000, Kulkarni 2009) and several attempts in whole structures (Tatsuo K 2009, Li 2012, Zhou 2013), the determination of the ranges of different types of elements still need further investigation since there's no any studies that have concerned with this issue yet.

Seismic damage of steel structures is related to several factors including structure forms, seismic attributes, section shapes etc. It is difficult to determine the application range for each kind of elements as it requires considerable work by taking every related factor into account. Consequently, the development of a simple and effective method to control the accuracy of multi-scale model is important. In this paper, multi-scale modeling work has been performed on structural members having the same section shape based on pushover analysis. The modeling results under seismic loading have proved the reliability and validity of the pushover analysis results to control the accuracy for multi-scale model. It also presents the modeling results for a steel arch bridge using both fiber model and multi-scale model. The necessity and applicability of multi-scale model for elasto-plastic seismic analysis of steel bridges has been discussed.

2. Investigation of accuracy for multi-scale model

2.1 Accuracy analysis based on pushover analysis

Section A and section B (Fig. 1) were used as examples to verify the practicability of the accuracy controlled by pushover analysis for structural members. Box section A has a dimension of 0.9 m×2.75 m, the thickness of its non-stiffened flange and stiffened web are 76 mm and 25 mm respectively, the diaphragm distance is 3.0 m. Box section B has a dimension of 0.8×0.8 m, the thickness of the steel plates is 25 mm, and the distance between diaphragms is 2.5 m.

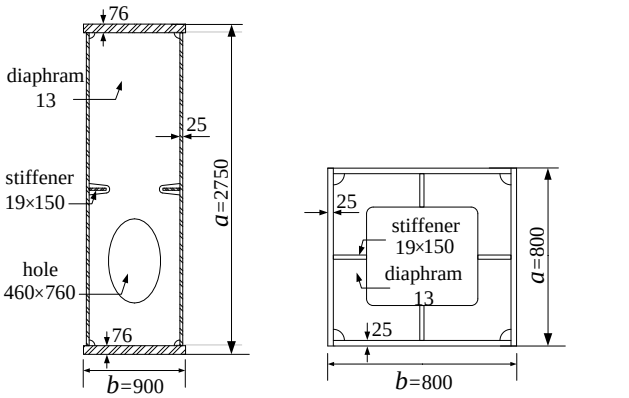

Fig. 1 Section type

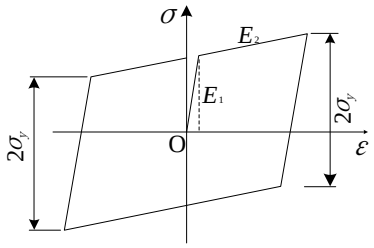

Fig. 2 Stress-strain relationship of steel material

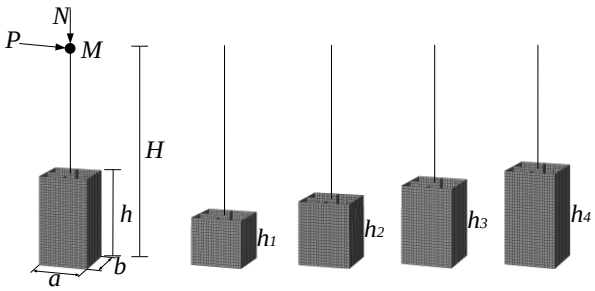

Fig. 3 The FE models for pushover analysis

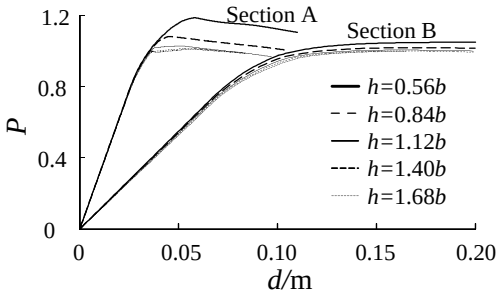

Fig. 4 Load-displacement curves of the members

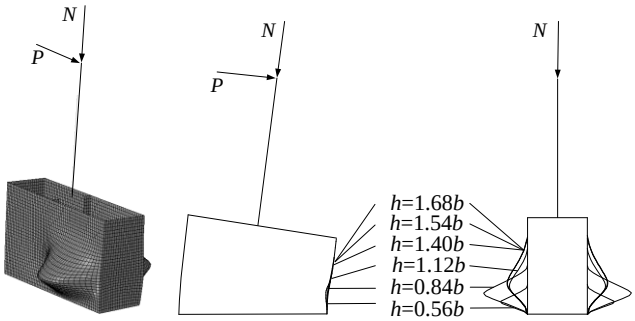

(a)Section A members

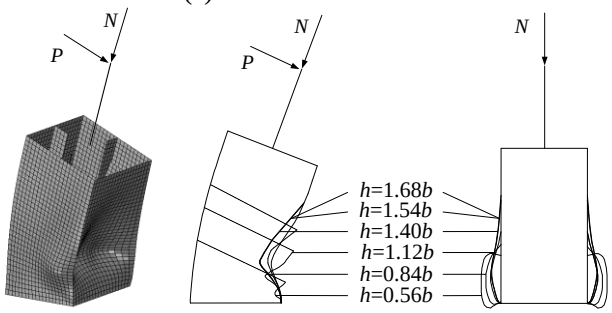

(b)Section B members

Fig. 5 Comparison of local deformations for the members

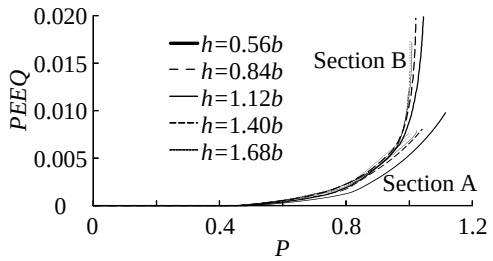

Fig. 6 Load-equivalent plastic strain curve of the fixed end

A bilinear stress-strain relation with kinematic hardening law as shown in Fig. 2 was adopted for steel material, the initial yield stress is 345MPa and the elastic young's modulus is 2.06×10^5MPa, the modulus after the yield point is taken as 1% of the initial one for the sake of the hardening of material.

Fig. 3 shows several multi-scale models of the cantilever member according to different division forms of shell and beam elements. As the plastic zone will concentrate in the fixed end for a cantilever member when subjected to a constant axial load N and a horizontal thrust P at the top, fine shell elements were used at the fixed end with a range height of h, while beam elements were used in the other part where will under a slight or no damage state. In order to compare the computational accuracy of different models, the length range of shell segment h varies from $0.56b$ to $1.68b$ (b is the width of the cross section) and the total height H of the member is $10b$. The

constant axial load N is taken as 0.3 times of the compressive yield axial force for the whole section N_y according to the service conditions of steel structures. The models and analysis were completed using FE package ABAQUS 6.10.

Fig. 4 shows the load P-displacement d curves at the top of the members obtained from pushover analysis. As can be seen, the curves of different models show similar behavior at the beginning, while differences were observed with the development of plasticity. When h has increased to 1.40b or longer, the load-displacement curves nearly coincide with each other indicating that the result has already get enough computational accuracy.

Fig. 5 shows the comparison of local deformation patterns for the cantilever members at the ultimate state. For comparison purpose, the figure in the left side shows a case obtained from a multi-scale model and the figure in the right side shows the local deformation contours of different models. It can be concluded that local deformations at the plastic areas are identical when the shell elements range length is larger than 1.40b, and the FE models can accordingly be considered as appropriate for the simulation of the local deformation process.

Fig. 6 shows the relationship between equivalent plastic strain (*PEEQ*) of the fixed end and the thrust P at the top. The result shows that shell model length h has little impact on equivalent plastic strain since there was no remarkable difference found with various value of h.

The comparison of pushover analysis for multi-scale models has proved that the convergence of the load-displacement curves can be used to estimate the accuracy of multi-scale models, there's no need to compare the other indices once the load-displacement curves become identical. For an increased value of the length for shell element segment, when there is little difference found between the obtained curves, the corresponding minimum height h can be adopted as the most reasonable length for the simulation of shell elements in a multi-scale model.

In addition, although the seismic damaged areas for complex bridges is associated with the dynamic axial force, the length for shell elements used in the FE model can be taken as the same as or slightly larger than the damage area. Strict consideration is not necessary for the actual dynamic axial force in the structures.

2.2 Accuracy of multi-scale model in seismic analysis

In order to evaluate the accuracy of multi-scale model with the proposed length of shell elements in nonlinear time history analysis for steel members, dynamic analysis was conducted for cantilever members with Hanshin earthquake recorded in Kobe University (1995), Chi-chi earthquake recorded near the Sun Moon Lake (1999) and Niigata earthquake recorded at Kawaguchi Machi (2004) as input seismic load in this part. Fig. 7 shows the acceleration waves of the earthquakes and their response spectra, the peak acceleration of Hanshin (HS), Chi-chi (CC) and Niigata (KWGC) waves were 8.12 m/s^2, 9.87m/s^2 and 16.75 m/s^2 respectively.

In order to improve the computational efficiency, the comparison was only carried out for the results between multi-scale model in which h=1.40b and full shell element model. Moreover, the seismic time history analysis was carried out with two structural forms whose fundamental periods were adjusted to 1.0s and 0.5s by changing the lumped mass at the top (Fig. 8).

As similar results were obtained for the analyses under different earthquake loads, this section only presents the seismic responses of structures with fundamental period of 1.0s under Hanshin earthquake. Fig. 9 shows the displacement-history curve of the top point on the members, where t is the ground motion time and d is the displacement. As can be seen, similar results were obtained

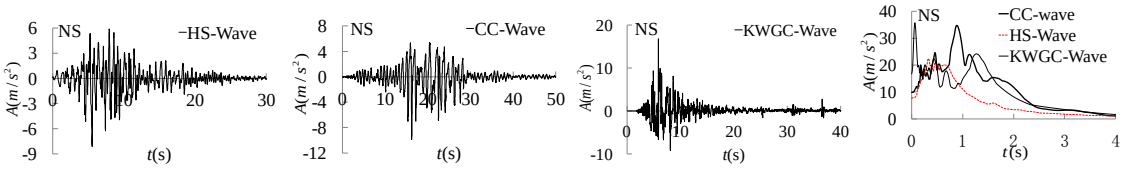

Fig. 7 Earthquakes input and response spectra

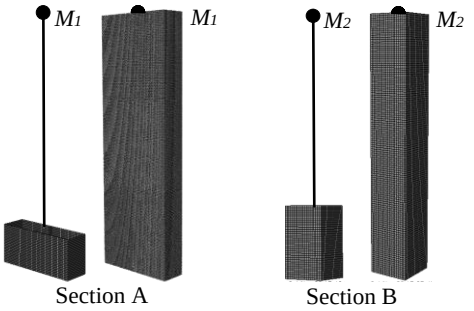

Fig. 8 FE models of the dynamic analysis members

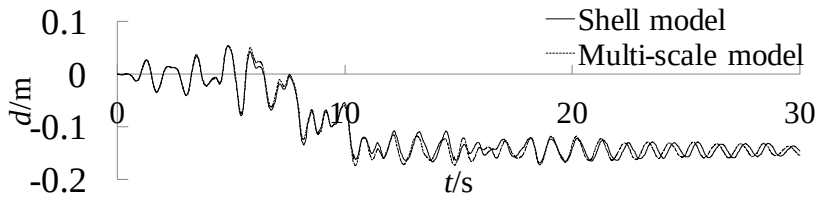

(a) Members with Section A

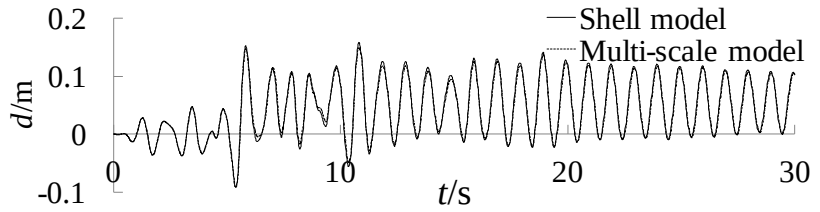

(b) Members with Section B

Fig. 9 Displacement-history curve of the free end

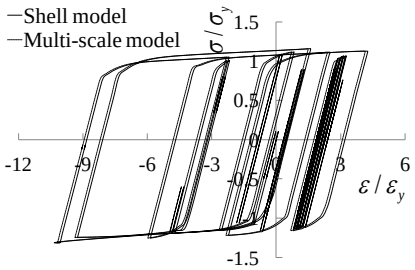

(a) Members with Section A

Fig. 10 Continued

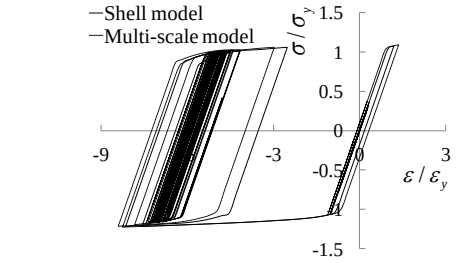

(b) Members with Section B

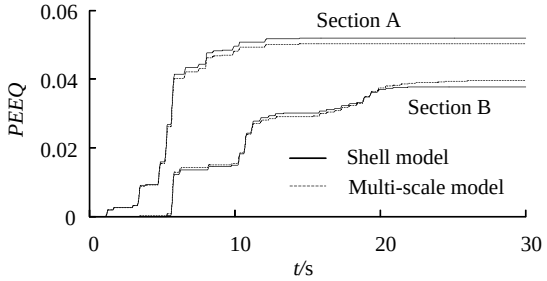

(c) PEEQ-history curve for the two members

Fig. 10 Stress-strain and PEEQ-history curve of the fixed end

for both the maximum and the residual seismic displacements.

Fig. 10 shows the stress-strain relationship and *PEEQ*-history curves of the fixed end on the members. As can be seen, multi-scale models have shown great accuracy for ductile evaluation in the seismic analysis of steel members.

As learned from preceding study, the load-displacement curves tend to coincide with each other as the increase of the length of shell elements segment. In particular, h =1.40b suggests a sufficient accuracy, which means the precision of multi-scale model can be ensured according to the convergence of load-displacement curves obtained from pushover analysis.

3. Seismic analysis of a complex steel bridge by multi-scale model

3.1 The bridge and earthquakes input

In this section, a deck-through type steel arch bridge was taken as an example, the results of seismic damaged area obtained using full fiber model and multi-scale model were compared, and the significance of seismic analysis by multi-scale model for complex steel bridge was discussed.

Fig. 11 shows a deck-through type steel arch bridge with a span length of 200 m and bridge deck width of 10m. The section type of the arch ribs and columns are the same with Section A and B shown in Fig. 1. In addition to the columns P3 and P14 are fixed with arch ribs and the girders at the two ends, the rest of the columns are all fixed with arch ribs and pinned to the girders. Nonlinear time history analysis was conducted with the structure between columns P3 and P14 since the expansion joints were set at its both ends. In order to consider the impact of different dynamic characteristics on the calculations, the analysis was carried out with both fixed and two-hinged arch structures.

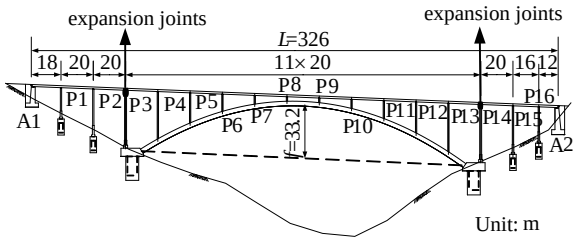

(a) Elevation of the bridge

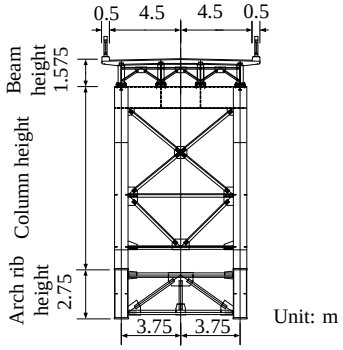

(b) Elevation of the column

Fig. 11 Design of the bridge structure

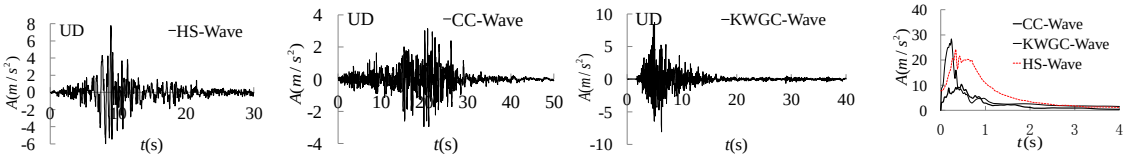

Fig. 12 Corresponding vertical earthquakes and their response spectra

The ground motions as shown in Fig. 7 were taken as longitudinal excitation and the corresponding vertical motions shown in Fig. 12 were used as the vertical excitation of the bridge to conduct the dynamic analysis, both material and geometric nonlinearity were considered.

3.2 The analytical models of bridge

Fig. 13 shows the multi-scale model and finite element meshes of some specific parts. Transverse braces were modeled by elastic beam elements as they do not suffer any damage from the earthquake, slightly seismic damaged parts like arch ribs or columns were modeled by fiber elements, and sever seismic damaged areas were modeled by fine shell elements. The length *h* for shell elements simulation of this model was taken as 1.40 times of the section width.

The transverse division of the section fibers for fiber elements is shown in Fig. 14, the steel plates were divided into two layers in the thickness direction, the sectional fibers was 775 and 783 in number for the two sections.

Fig. 15 shows the three dimensional full fiber model of the arch bridge whose sectional fiber

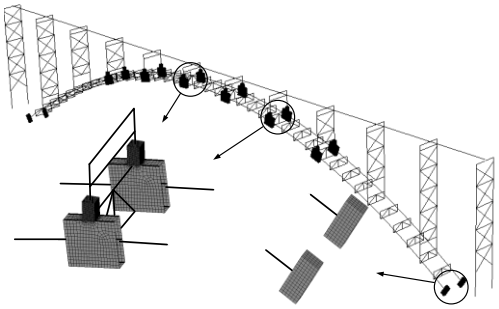

Fig. 13 Multi-scale model of the structure

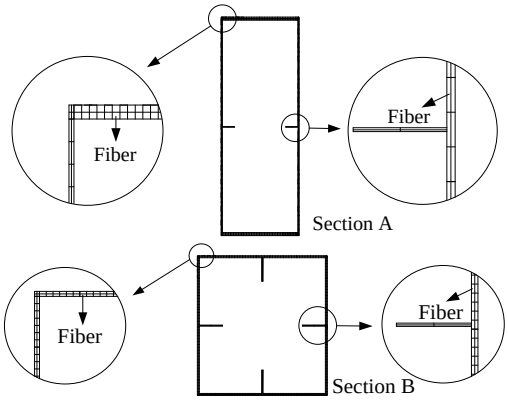

Fig. 14 The division of the section fibers

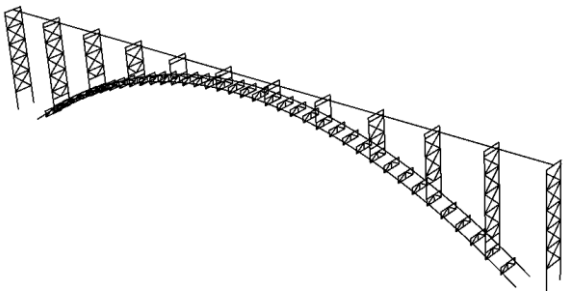

Fig. 15 Fiber model of the structure

division was the same as that of multi-scale model, and the fiber model was also refined in the anticipated seismic damaged areas.

3.3 Stress distribution and free vibration characteristics at the completed bridge state

Fig. 16 shows the axial stress at the 1/4 span of the arch rib under the completed bridge state for the two models. The comparison results obtained from two-hinged arch structure are similar

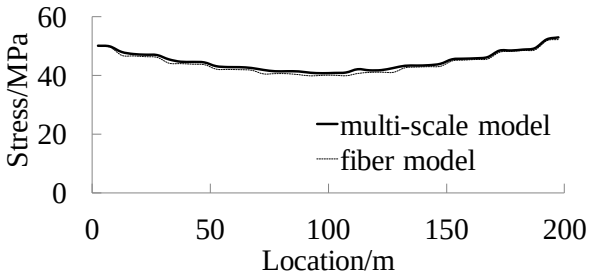

Fig. 16 Stress of the fixed arch bridge under completed bridge state

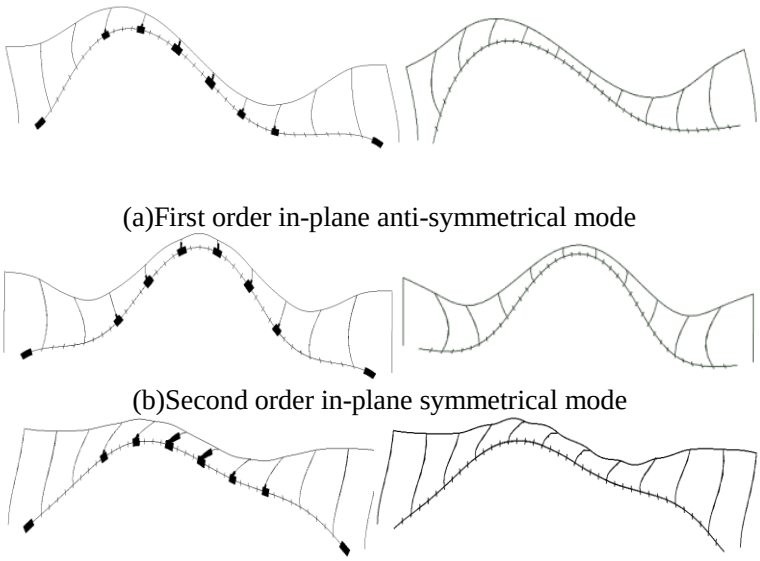

(a)First order in-plane anti-symmetrical mode

(b)Second order in-plane symmetrical mode

(c)Third order in-plane anti-symmetrical mode

Fig. 17 Comparison of lower order vibration modes of different models

Table 1 Natural vibration period of arch bridges

Structure form	Lower order in-plane vibration mode	T_m/s	T_f/s	Maximum difference/%
Two-hinged arch structure	First order	2.315	2.307	0.3
	Second order	0.979	0.979	0.0
	Third order	0.559	0.552	1.3
Fixed arch structure	First order	1.481	1.474	0.5
	Second order	0.763	0.761	0.3
	Third order	0.543	0.531	2.3

with that of fixed arch bridge. The initial stresses distribution obtained from the two models are similar with each other.

Based on the tangent stiffness at the completed bridge state, the free vibration characteristics can be calculated from the equation:

$$\left|\boldsymbol{K}_{\mathrm{e}}+\boldsymbol{K}_{\mathrm{G}}-\omega^{2}\boldsymbol{M}\right|=0 \tag{1}$$

where $\boldsymbol{K}_{\mathrm{e}}$ is the elastic stiffness matrix of the structure, $\boldsymbol{K}_{\mathrm{G}}$ is the geometric stiffness matrix corresponding to the initial stress, ω is the eigenvalue of vibration and $\boldsymbol{M}$ is mass matrix. Table 1 compares free vibration period of the steel bridges, where T_m and T_f stand for the periods obtained from multi-scale model and fiber model respectively. The results show that the dynamic characteristics are quite similar, the maximum difference of the frequencies corresponding to lower order vibration modes between the two models is less than 3%.

Fig. 17 only shows the lower order in-plane vibration modes of the fixed arch bridge since the mode shapes of fixed and two-hinged arch structures are similar. The results indicate the lower order vibration modes calculated from both kinds of models are also the same.

The comparison of the stresses and free vibration characteristics for the two models at their completed bridge state shows that the stiffness and mass distributions of the two models are similar, and the mechanical behavior in linear elastic range could be considered as identical for two different models.

3.4 Comparison of the seismic results

3.4.1 Comparison of displacement-history curve

Consistent modeling results have been obtained for fixed and two-hinged arch structures, Fig. 18 shows the displacement-history comparison at the 1/4 span on the arch rib of the bridge under Chi-chi earthquake. The displacement response of multi-scale and fiber models is quite similar, and fiber model can represent the global seismic response of the structure accurately.

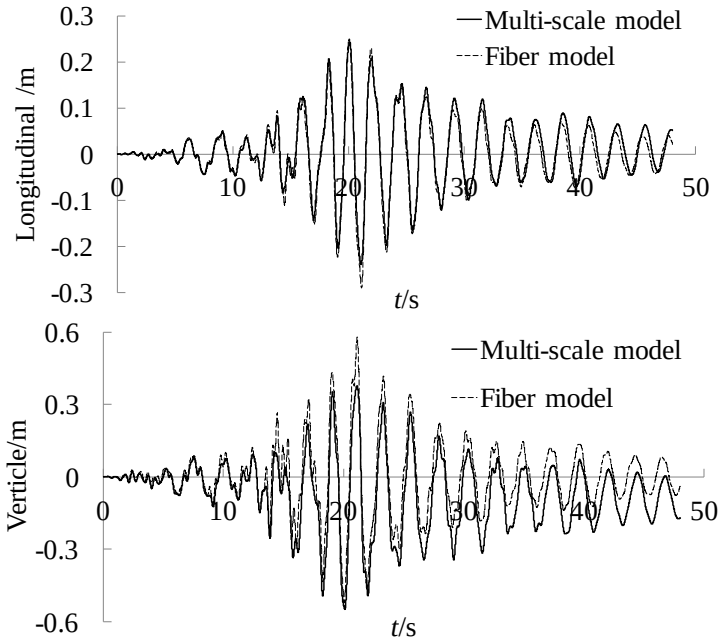

Fig. 18 Displacement-history curve of 1/4-span arch rib under Chi-chi earthquake

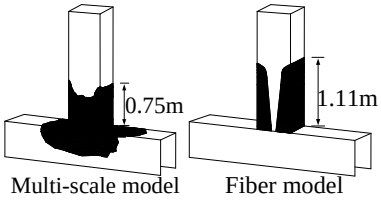

(a)Results under Chi-chi earthquake

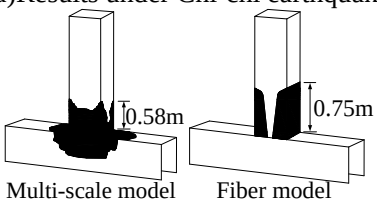

(b) Results under Kobe earthquake

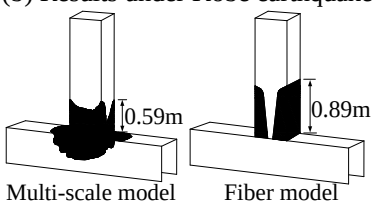

(c) Results under Niigata earthquake

Fig. 19 Plastic region at the bottom of P8 column on fixed arch bridge

3.4.2 Comparison of seismic damaged area

All the seismic damaged areas obtained from the two models concentrate at the joints of columns and arch ribs that close to the mid-span. The bottom of columns P8 & P9 shows a severe degree of damage, and slight damage was found at the bottom of columns P6, P7, P11 & P12.

Fig. 19 shows the size of plastic region at the bottom of column P8. As can be seen, though different patterns were observed, plasticity has developed at the same location of fixed and two-hinged arch bridges when subjected to a certain earthquake. The size of seismic damaged areas shows great difference between the two models. The plasticity obtained from multi-scale model distributed through the whole section of column P8 and extended to the adjacent arch rib, while plastic area predicted by fiber model only concentrated on column with a larger distribution. The above results demonstrate that fiber model have a lack of accuracy for the prediction of plasticity and it is necessary to build a multi-scale model to consider the seismic damage process of steel bridge. Moreover, though the length of the plastic area in column is larger than that in arch rib, it is still shorter than 1.40times of the column section width, which meets the proposed requirement of the study described in previous section for multi-scale model.

3.4.3 Local deformation of the structure

The most obvious local deformations were observed at the same positions as plasticity occured, Fig. 20 shows the maximum local deformation at the bottom of column P8 under Chi-chi earthquake. It can be seen that obvious local deformation located at the seismic damaged area of the steel structure, and the plane cross-section assumption was not satisfied any more, which

indicated the results from fiber model were unreliable. However, it is noted that local deformation and seismic plasticity only developed at the joints of bridges, the length of their region was less than 1.40*b*, which means the control index of multi-scale model based on pushover analysis is practical.

3.4.4 Comparison of plastic strain

Fig. 21 shows the stress-strain curve of two-hinged arch bridge at the bottom of columns P7, P8 and P9. The results show a significant difference between different models, fiber model shows a higher precision when the seismic damage is slighter. However, there is a decrease trend for the precision of fiber model as the development of local deformation, which indicate that fiber model can only evaluate the slight seismic damage of steel bridge and the deficiency can be overcome by the multi-scale model.

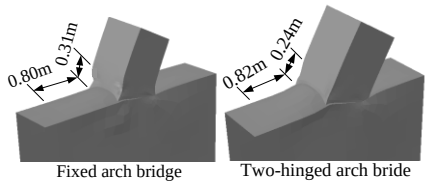

Fig. 20 Local deformation of arch bridges

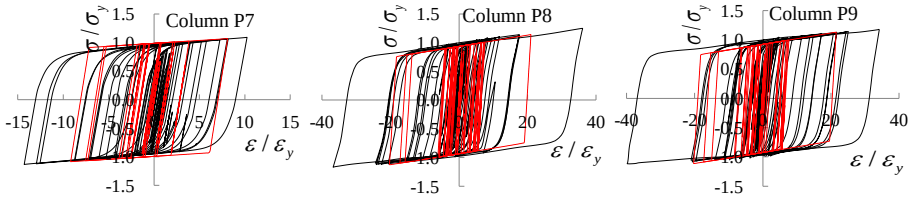

(a)Results under Chi-chi earthquake

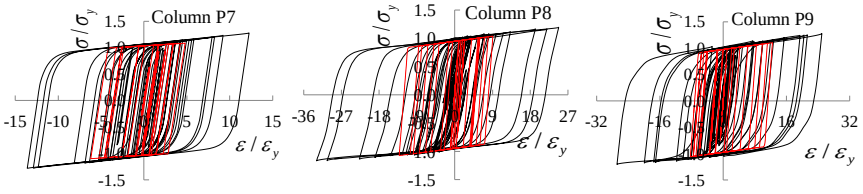

(b) Results under Kobe earthquake

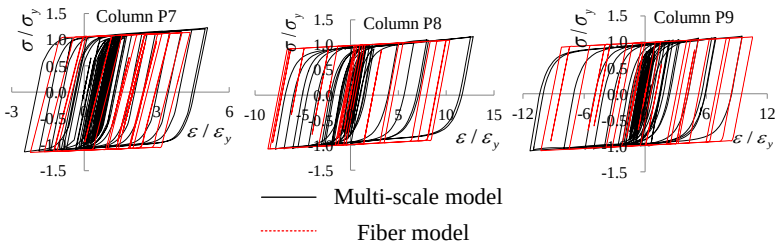

(c) Results under Niigata earthquake

Fig. 21 Stress-strain curve at the bottom of P8 column on two-hinged arch bridge

5. Conclusions

This paper proposed an efficient method to establish multi-scale models based on pushover analysis of structural members having the same section pattern, and examined the validity and the necessity in elasto-plastic seismic response analysis for complex steel bridges. The following conclusions can be drawn from this study.

- The computational accuracy in static and dynamic analysis of multi-scale model can be verified according to the convergence of the load-displacement curves for members sharing the same section pattern by pushover analysis.
- The case study described in this paper shows that once the length of shell elements segment in structures is larger than 1.40 times of the section width, the appropriate accuracy in static and dynamic analysis of the model can be expected.
- Fiber model can only predict the global seismic deformations and approximate positions of the damaged areas during the dynamic analysis, but it cannot provide accurate information for the size and degree of the damaged areas.
- Multi-scale model shows good performance for the predictions of both the global deformations and the seismic damage process, which is superior to fiber model, and it also has a higher computational efficiency than full shell model.

A universal determination of seismic damaged length of a stiffened steel box column still needs a further study with varieties of different section types.

Acknowledgement

The author would like to appreciate the financial support of National Natural Science Foundation of China (51378460).

References

Nonaka, T. and Ali, A. (2001), "Dynamic response of half-through steel arch bridge using fiber model", *J. Bridge Eng*., ASCE, **6**(6), 482-488.

Liang, C.Y. and Chen, A. (2010), "A method for examining the seismic performance of steel arch deck bridges", *Front. Archit. Civil Eng. China*, **4**(3), 311-320.

Usami, T, Lu, Z, Ge, H. and Kon, T. (2004a), "Seismic performance evaluation of steel arch bridges against major earthquakes", Part 1: Dynamic analysis approach, *Earthq. Eng. Struct. Dyn*., **33**(14), 1337-1354.

Lu, Z., Tsutomu Usami, T. and Ge, H. (2004b), "Seismic performance evaluation of steel arch bridges against major earthquakes", Part 2: Simplified verification procedure, *Earthq. Eng. Struct. Dyn*., **33**(14), 1355-1372.

Cetinkaya, O.T., Nakamura, S. and Takahashi, K. (2006), "A static analysis-based method for estimating the maximum out-of-plane inelastic seismic response of steel arch bridges", *Eng. Struct*., **28**(5), 635-647.

Xie, X., Lin, G., Duan, Y.F. and Zhao, J.L. (2012), "Seismic damage of long span steel tower suspension bridge considering strong aftershocks", *Earthq. Struct*., **3**(5), 767-781.

Kawashima, K. and Unjoh. S. (1997), "The damage of highway bridges in the 1995 Hyogo-Ken Nanbu Earthquake and its impact on Japanese seismic design", *Earthq. Eng*., **1**(3), 505-541.

Zheng, Y., Usami, T. and Ge, H.B. (2000), "Ductility of thin-walled steel box stub-columns", *J. Struct. Eng*., **126**(11)**,** 1304-1311.

Usami, T. (2007), "Guidelines for seismic and damage control design of steel arch bridges", Tokyo: GIHODO SHUPPAN Co. Ltd. (In Japanese)

Ge, H. and Tsumura, Y. (2009), "Experimental and analytical study on the evaluation of ductile crack initiation in steel bridge piers", *J. Struct. Eng., JSCE*, **55A**, 605-616.

Specifications for highway bridges, Part V: Seismic Design. Tokyo, Japan, 2002.

Alvarez, J., Aparicio, A., Jara, J. and Jara, M. (2012), "Seismic assessment of long-span arch bridge considering the variation in axial forces induced by earthquakes", *Eng. Struct.*, **34**, 69-80.

Goto, Y., Qingyun, W. and Obata, M. (1998), "FEM analysis for hysteretic behavior of thin-walled columns", *J. Struct. Eng.*, **124**(11), 1290-1301.

Hanbin, G., Shengbin, G. and Usami, T. (2000), "Stiffened steel box columns. Part 1: Cyclic behavior", *Earthq. Eng. Struct. Dyn.*, **29**(11), 1691-1706.

Usami, T., Shengbin, G. and Hanbin, G. (2000), "Stiffened steel box columns. Part 2: Ductility evaluation", *Earthq. Eng.Struct. Dyn.*, **29**(11), 1707-1722.

Kulkarni, N.G., Kasai, A. and Tsuboi, H. (2009), "Displacement based seismic verification method for thin-walled circular steel columns subjected to bi-directional cyclic loading", *Eng. Struct.*, **31**(11), 2779-2786.

Tatsuo, K., Akira, K. and Saeki, I. (2009), "Seismic performance evaluation of steel continuous bridges with rigid superstructure-pier connections[J]", *J. Struct. Eng., JSCE*, 55A, 564-572. (In Japanese)

Li, Z.X., Jiang, F.F. and Tang, Y.Q. (2012), "Multi-scale analysis on *seismic* damage and progressive failure of steel structures", *Finite Elem. Anal. Des.*, **48**(1), 1358-1369.

Zhou M., Nie J. and Fan J. (2013), "Multi-scale analysis of the steel cable anchorage system of self-anchored suspension bridges", *Structure Congress 2013, ASCE*, 467-478.

IT